

# 特集 Noise Robust Optical Sensor for Driver's Vital Signs\*

二ツ山幸樹

Kouki FUTATSUYAMA

光本直樹

Naoki MITSUMOTO

河内泰司

Taiji KAWACHI

中川 剛

Tsuyoshi NAKAGAWA

We have developed a built-in vital sign sensor, which allows drivers to noninvasively measure their heartbeat and pulse wave just by gripping the steering wheel in the usual manner. Unlike conventional vital sign sensors used in clinical practice, such as an electrocardiogram sensor for measuring the heartbeat and photoplethysmogram sensor for measuring the pulse wave, our system requires no preparation or gel. One of the major issues we have successfully addressed is the suppression of mechanical vibration and electrical noise affecting the pulse wave sensor, which is far more susceptible to disturbances than heartbeat monitoring, especially while driving. To address this issue we have developed several new techniques: an active type optical sensor using a 525 nanometer green light-emitting diode which enhances the signal-to-noise ratio (SNR) of the pulse wave signal, an anti-vibration mounting mechanism for the sensor module which reduces vibration from the steering wheel, and a heartbeat signal-triggered ensemble averaging signal processing technique to recover a clean pulse wave from a noisy signal. As a result, we successfully achieved a 27 dB improvement in the SNR and have succeeded in recovering a clean 42 dB pulse wave from a noisy signal while the driver is at the wheel.

## 1. INTRODUCTION

Health-related accidents are becoming one of the biggest concerns in aging societies like Japan. The number of traffic accidents in Japan caused by senior drivers aged 65 years or older has increased 1.84-fold, from 62,672 (out of 815, 812 accidents in total) to 104,870 (out of 697,285 accidents in total) in the decade between 1999 and 2009, while the number of accidents by younger drivers between 16 and 24 years has actually reduced 0.57-fold, from 188,656 to 107,628, over the same period<sup>1)</sup>. Similarly, the number of driver's license holders 65 years or older has increased 1.8-fold, from 6,785,000 (out of 74,793,000 in total) to 12,471,000 (out of 80,812,000 in total) between 1999 and 2009, while the number of younger license holders has reduced 0.72-fold from 9,067,000 to 6,535,000 over the same period. Senior drivers are very susceptible to diseases such as dementia, syncope or heart attacks while driving, and since they are more likely to become incapable of driving safely they can cause very serious accidents. Detecting any unusual and abnormal health conditions and quickly assisting or intervening effectively in the person's driving is one of the key factors in reducing the incidence and severity of such accidents. To address this issue, we are currently working on a system to monitor the driver's heartbeat and pulse wave as the first step in establishing a driver's vital sign-based vehicle safety system. These vital signs can be reliably measured

clinically using electrocardiogram and photoplethysmogram sensors. The electrocardiogram sensor detects tiny electrical changes on the skin caused by the heart muscle activity, and the photoplethysmogram sensor illuminates the skin and measures changes in light absorption due to blood flow under the skin. However, these medical sensors are limited in terms of availability and operating conditions, and while they are suitable for in-hospital usage they are not suitable for in-vehicle use. The medical electrocardiogram sensor requires patients to have gel applied to their skin and electrodes must be carefully attached to specific parts of the body, while the medical photoplethysmogram sensor requires patients to maintain a consistent posture and a constant contact force between the skin and the sensor to avoid disturbing or blocking the blood flow. We needed to modify these medical sensors to make them suitable for in-vehicle usage, and one of the biggest challenges was to obtain a clean pulse wave signal under noisy in-vehicle conditions. The photoplethysmogram sensor is far more susceptible to these disturbances than the electrocardiogram sensor. Julian M. Goldman and Michael T. Petterson proposed the use of a motion artifact reduction technique for a photoplethysmography-based pulse oximetry sensor in which new adaptive filtering techniques compute motion artifact and remove them from the sensor signals<sup>2)</sup>. However, this technique only reduces motion artifact problems effectively if the con-

\*Reprinted with permission from SAE paper 2011-01-1024 Copyright © 2011 SAE International.

tact force between the person’s hand and sensor is maintained at a constant level. H. J. Baek and H. B. Lee proposed an in-vehicle vital sign monitoring system that would monitor multiple vital signs, including the electrocardiogram and the pulse wave<sup>3)</sup>. However, their interest was to assess driver stress rather than to build a sensor system, and no techniques were proposed to tackle real-world noise problems. This paper focuses on the techniques needed to maintain an adequate contact force on the photoplethysmogram sensor and to obtain a clean pulse wave signal under in-vehicle conditions.

## 2. OVERVIEW OF OUR STEERING WHEEL SENSOR

First, we defined the requirements for our steering wheel sensor as shown in **Table 1**. One of the significant requirements is to obtain a driver’s vital signs without his or her awareness. Another significant requirement is to obtain clean sensor signals of both electrocardiogram (ECG) and pulse wave under driving conditions. While driving, vehicle vibration is the most serious problem, because it causes unstable contact between the sensor and the driver, which deteriorates the sensor signals significantly. We measured vehicle vibration on several roads and found vehicle vibration of 0.6 m/s<sup>2</sup> was the worst-case condition. The SNR of the ECG requires more than 10 dB because it is analyzed only to determine its peak. On the other hand, the SNR of the pulse wave requires more than 40 dB, because the pulse wave is analyzed to extract several features, such as the acceleration plethysmograph<sup>4)</sup>, which enables us to estimate the driver’s condition.

Table 1 Requirements of our steering wheel sensor

Driver’s awareness during measurement	Not required
SNR of ECG under vehicle vibration of 0.6 m/s <sup>2</sup>	10 [dB]
SNR of pulse wave under vehicle vibration of 0.6 m/s <sup>2</sup>	40 [dB]

In order to satisfy the requirement that the driver should not be aware of the measurement process, we developed a steering wheel sensor system. Our newly developed sensor system, which consists of a chrome-coated electrode, an LED, a photodiode and a CPU, allows drivers to monitor their heartbeat and pulse wave signal while driving (**Fig. 1**). The measurement is obtained by simply gripping the steering

wheel with both hands, and no gel or other extra equipment is required. **Table 2** shows the specifications of our steering wheel sensor.

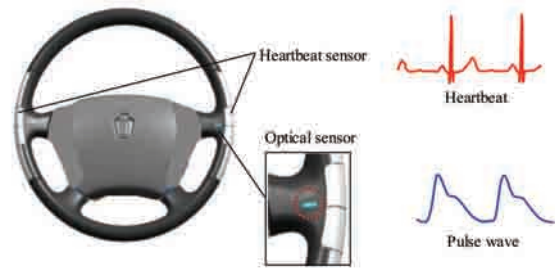


Fig. 1 Newly developed steering wheel sensor. The right and left sides of the steering wheel are covered with chrome-coated electrodes that serve as the heartbeat sensor. If a driver grips both electrodes, the driver’s body completes the electrical circuit and enables the system to measure heartbeat signals. The optical sensor, installed on the right-hand side of the steering wheel, consists of an LED and a photodiode. If the driver’s palm comes into contact with this sensor, it measures blood flow change due to pulsation by emitting light with a wavelength of 525 nanometers and receiving reflected light. Neither gel nor any other form of preparation is required.

Table 2 Specifications of our steering wheel sensor

Heartbeat sensor	principle	electrocardiograph-based
	electrode	chrome-coated, 90 k ohm (contact impedance)
	input impedance	1000 k ohm
	gels	not required
Pulse wave sensor	principle	photoplethysmograph-based
	light emitting device	525 nanometers (green wavelength) 360 microwatts (power)
	A/D converter	frequency: 1000 Hz. resolution: 10 bits

As shown in **Fig. 2**, two pairs of chrome-coated electrodes are located on the steering wheel. One pair of electrodes is placed on the right-hand side of the steering wheel, where drivers normally grip the wheel, and the other pair of electrodes corresponds to the driver’s left-hand placement. Each pair of electrodes is composed of a ground electrode and a signal electrode. When the driver grips the steering wheel with both hands, the driver’s body and the steering wheel are coupled together electrically, enabling the system to measure the driver’s heartbeat. This sensing principle is equivalent to that used by medical electrocardiogram sensors. Unlike these conventional medical heartbeat sensors, which need gel to reduce contact impedance between the skin and the electrode, our sensor does not require the use of gel because the input impedance of the circuit is designed to be high enough to receive an adequate signal even from dry electrodes.

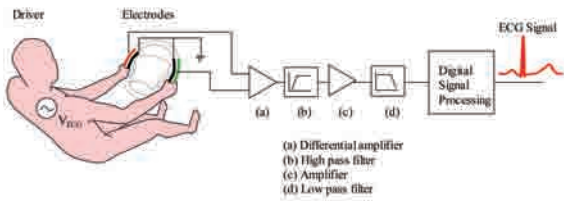


Fig. 2 Circuit diagram for the heartbeat sensor. The sensor is composed of two pairs of chrome-coated electrodes, a differential amplifier, a high pass filter and a low pass filter.  $V_{ECG}$  represents the signal source of the electrocardiogram generated by the human body. By gripping the steering wheel with both hands, the human body and the steering wheel create a closed circuit that works as an electrocardiogram (ECG) sensor. Baseline wander, which is considered as an artifact caused by perspiration, respiration, body movements and poor electrode contact, is removed by a high pass filter with a cutoff frequency of 0.3 Hz, and noise is removed by a low pass filter with a cutoff frequency of 35 Hz. The output of the analog circuit then enters a digital signal processing circuit and is digitized at a sampling frequency of 1000 Hz and a resolution of 10 bits. The waveform shown by the red line represents a typical electrocardiogram waveform.

As shown in Fig. 3, the optical sensor consists of a photodiode, an LED, an acrylic lens, and a current-voltage conversion circuit. Light with a wavelength of 525 nanometers at 360 microwatts is emitted from the LED, penetrates the skin on the driver’s palm, reflects off the artery under the skin, bounces back and reenters the photodiode. The pulsation of the blood flow causes the blood volume within the vessels to alter, thereby changing the light absorbance and affecting the signal power received back at the photodiode (Fig. 3). This technique is equivalent to that used in photoplethysmography, which is widely used to monitor a patient’s pulse wave while undergoing surgery.

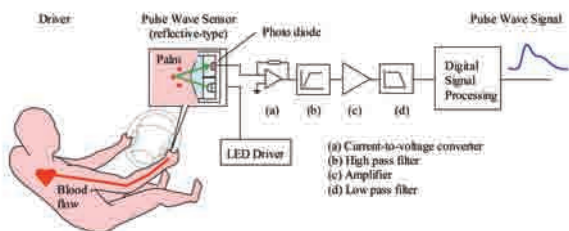


Fig. 3 Circuit diagram for the pulse wave sensor. The LED emits light with a wavelength of 525 nanometers at 360 microwatts. The light penetrates through the skin to the artery, and then bounces off back to the photodiode. The photodiode detects blood flow changes, which closely correspond to the natural pulsation of blood flow. Baseline wander is removed by a high pass filter with a cutoff frequency of 0.3 Hz, and noise is removed by a low pass filter with a cutoff frequency of 30 Hz. The output signal from the analog circuit then enters a digital circuit and is digitized at a sampling frequency of 1000 Hz and a resolution of 10 bits. The waveform shown by the blue line represents a typical pulse wave signal.

### 3. TECHNIQUES TO IMPROVE SNR UNDER NOISY CONDITIONS

One of the major issues to be addressed in order to make our steering wheel sensor effective while driving was the problem of obtaining a robust, high signal-to-noise ratio (SNR) signal under noisy conditions. We conducted an experiment to assess to what degree the SNR of the signal deteriorated under typical driving conditions. As shown in Fig. 4, we found that the SNR of the pulse wave deteriorated significantly by up to 19 dB at a vehicle speed of 80 km per hour and up to  $0.65 \text{ m/s}^2$  vertical vehicle acceleration, while the SNR of the electrocardiogram only deteriorated by 8 dB under the same conditions.

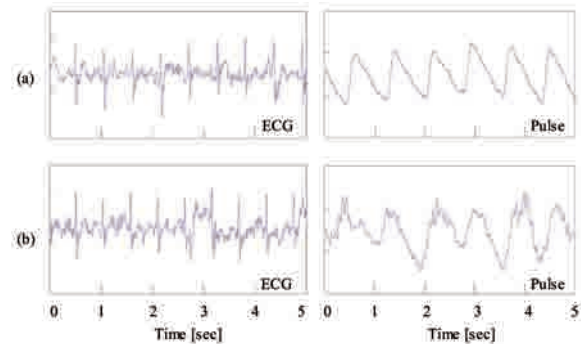


Fig. 4 Conventional medical sensor performance under noisy conditions. The (a) upper and (b) lower figures were obtained in a stationary vehicle and in a moving vehicle, respectively. The moving vehicle was experiencing  $0.65 \text{ m/s}^2$  vertical vehicle acceleration at 80 km/h. The SNR of the pulse wave deteriorated significantly by up to 19 dB, from 34 dB to 15 dB, while that of the ECG deteriorated by only 8 dB. This result indicates that the pulse waveform was far more susceptible to disturbances than the ECG.

We found that the major cause of pulse wave deterioration was contact force fluctuation between the optical sensor and the skin on the palm of the hand. As shown in Fig. 5, contact force fluctuation changes blood flow, altering light absorption and affecting the pulse waveform. This result indicates that the contact force must be maintained at 0.1 N even if the vehicle is vibrating while driving. In order to design a mechanism that could maintain a contact force ( $F$ ) up to 2.0 N, we modeled the mechanical linkage of the optical sensor head and steering wheel, as shown in Fig. 5. The key issue here was to obtain a spring constant,  $k_1$ , which satisfied  $F$  up to 1.0 N. The symbols shown in Fig. 5 are as follows:  $k_0$ ,  $C_0$  and  $M$  are the spring constant, damping coefficient and the mass of the driver’s hand, respectively, while  $m$  is the mass of the optical sensor head, and  $k_1$  is the

constant for the spring that links the steering wheel and optical sensor. Using this model, we obtained a value of 200 [N/m], when  $k_0 = 600$  N/m,  $C_0 = 400$  Ns/m,  $M = 1$  kg, and  $m = 1$  g. Figure 6 demonstrates the performance of our mechanism, showing how the standard deviation for the contact force fluctuation was successfully reduced by up to 14% compared with the same mechanism without the spring (the standard deviation of the proposed mechanism was 0.05 N and that without the spring was 0.37 N). The maximum contact force of the proposed mechanism was successfully maintained 0.82 N, small enough to avoid waveform deterioration, however, that without the spring was 2.0 N.

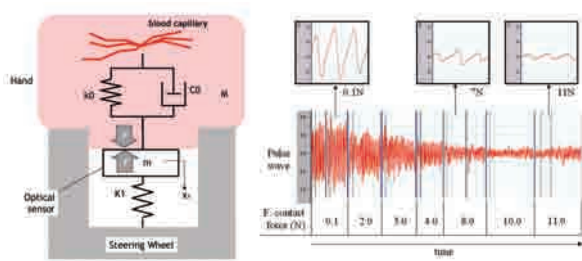


Fig. 5 Relationship between contact force  $F$  and the pulse waveform.  $F$ , in the left-hand figure, is the contact force between the skin and the optical sensor unit. The right-hand figure demonstrates how contact force affects the pulse waveform. Increasing the contact force from 0.1 to 11.0 N causes the pulse waveform to deteriorate, and the best waveform is obtained when the contact force is 0.1 N. This result indicates that the contact force must be maintained around 1.0 N, even if the vehicle vibrates while driving.

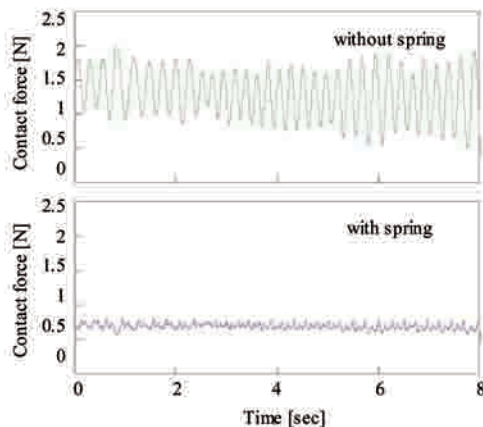


Fig. 6 Effect of the proposed mechanism. The (a) upper and (b) lower graphs were obtained by a mechanism without and with a spring, respectively. By using a spring with a spring constant,  $k_1$ , of 200 N/m we successfully maintained a maximum contact force of 0.83 N and kept the fluctuation in contact force to 0.05 N.

We also employed a homogeneous ensemble-averaging signal processing technique to recover a clean pulse waveform from noisy sensor signals<sup>5)</sup>. The issue here was to obtain the correct trigger timing because the accuracy of the trigger timing greatly affects the performance of the ensemble averaging technique. The left side in Fig. 7 shows the electrocardiogram signal and pulse waveform measured under actual in-vehicle driving conditions, and the right side in the figure demonstrates the recovered pulse wave obtained by the ECG-triggered ensemble averaging technique. We concluded that using the electrocardiogram signal as a trigger improves the performance of ensemble averaging, overall.

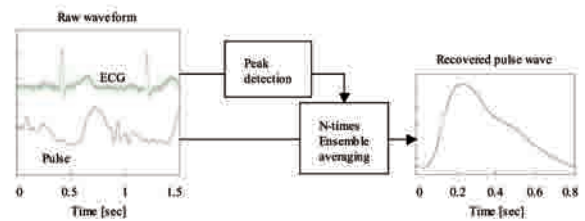


Fig. 7 ECG-triggered ensemble averaging for pulse waveform

#### 4. TEST RUN WITH A CAR

We conducted experiments to assess the performance of our spring mechanism and the heartbeat-triggered ensemble averaging technique. The experiments were conducted by driving on a rough asphalt road in our test course. The tests were performed at three vehicle speeds of 40km/h, 60km/h and 80km/h. Table 3 illustrates the experimental results with vehicle velocity, vehicle vibration and SNR with (a), (b) and (c) representing the pulse waveform measured without either the spring or ensemble averaging, the waveform measured with the spring only, and with both spring and ensemble averaging, respectively. The results show that the SNR with (a) deteriorated to 15 dB under vehicle vibration of  $0.65\text{m/s}^2$ . Under such a noisy condition, our techniques successfully improved pulse waveform quality by up to 27 dB, from 15dB to 42 dB in terms of the SNR, which satisfies the requirement in Table 1. Fig. 8 illustrates waveforms obtained under vehicle speed of 80km/h, with (a), (b) and (c). These waveforms demonstrate the restoration of the pulse wave by the application of our technique.

Table 3 Results of the test run with a car

vehicle speed [km/h]	SNR [dB]			vehicle vibration [m/s <sup>2</sup> ]
	[a]	[b]	[c]	
40	24	34	47	0.34
60	21	32	44	0.49
80	15	29	42	0.65

(a), (b) and (c) represent the pulse waveform measured without either spring or ensemble averaging, with the spring only, and with both spring and ensemble averaging, respectively. The vibration was measured by NAV440<sup>6)</sup> manufactured by Crossbow Technology, Inc. and calculated as the root mean square of the vertical vehicle acceleration. The SNR was calculated by a commonly used equation<sup>7)</sup>. In ensemble averaging, 20 pulse wave sets were averaged. Under vehicle vibration of more than 0.6 m/s<sup>2</sup>, the SNR was improved by more than 40dB, which satisfies the requirement for pulse wave SNR in Table 1.

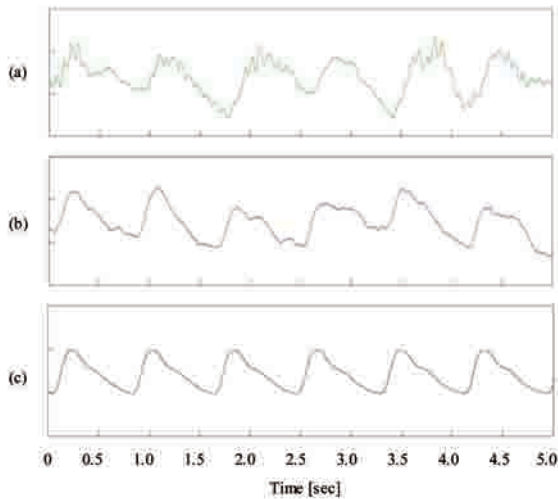


Fig. 8 The performance of our spring mechanism and ensemble averaging technique: (a), (b) and (c) represent the pulse waveform measured without either spring or ensemble averaging, with the spring only, and with both spring and ensemble averaging, respectively (at a vehicle speed of 80 km/h). The SNR of (a) (b) and (c) was 15 dB, 29 dB and 42 dB, respectively. This result proved that our technique successfully improved pulse waveform quality by up to 27 dB, from 15 dB to 42 dB.

### 5. BLOOD PRESSURE ESTIMATE – POTENTIAL APPLICATION

Another potential application of the pulse wave sensor that we are currently developing is a real-time blood pressure monitoring system. Fig. 9 shows the proposed system in diagrammatic form. First, from 752 test subjects, we built up a database that is composed of pulse wave signals measured by the proposed sensor and blood pressure data measured by a cuff-type blood pressure sensor<sup>8)</sup>. Table 4 shows

the features of the database. By learning from the database using a stepwise multiple regression method<sup>9)</sup>, we constructed a model to estimate person’s blood pressure from the pulse waveform. As shown in Fig. 10, we were able to estimate blood pressure with an error of less than 4.3 +/- 2.4 [mmHg]. The input data for this demonstration were measured at a vehicle speed of 100 km/h.

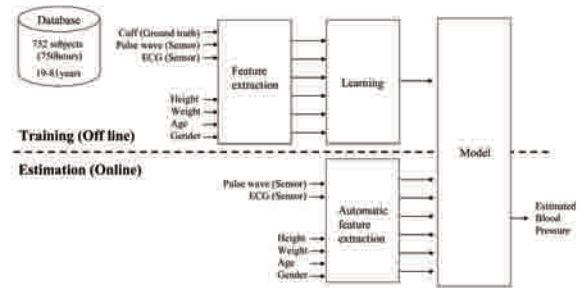


Fig. 9 System schematic of blood pressure estimation. The estimation model was obtained by learning from the pulse wave database that included data from 752 test subjects. Using this model, the system estimates blood pressure from the pulse wave signal.

Table 4 Features of the database

Subject	Number	752 (Male:431, Female: 321)
	Age	Mean: 53.0 years old Standard deviation: 18.6 years old
Measurement instrument	ECG	Steering wheel sensor
	Pulse wave	
	Blood pressure	Cuff-type (Electronic Sphygmomanometer)
Measurement condition	State	Relaxed
	Posture of the Subject	Seated posture
	Environmental temperature	25 degrees C

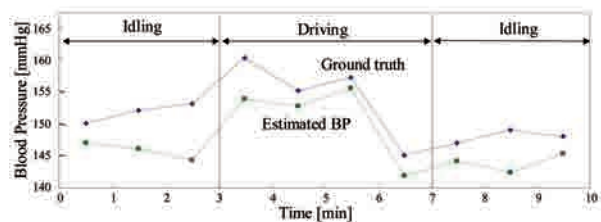


Fig. 10 The performance of blood pressure estimation under in-vehicle conditions. We successfully estimated blood pressure with an error of less than 4.3 +/- 2.4 [mmHg] at a vehicle speed of 100 km/h on a paved road in our test course. We intended to assess both the blood pressure itself and blood pressure variation. Therefore, we chose a vehicle speed of 100 km/h to induce variations in the driver’s blood pressure. The decision was made to use a paved road to ensure driver safety at a vehicle speed of 100 km/h.

6. FUTURE VISION

This chapter presents our ideas on how data from the driver's vital sign sensors could be applied to enhance the safety and comfort of vehicles in the future. Fig. 11 shows how the daily health check system could work, in practice. We have assumed that many drivers use their car each day for commuting, shopping or picking up their children and these routine behaviors could be quite useful for accumulating data on the everyday health of drivers. Our daily health check system will, therefore, be activated just after the driver gets into their car, the system will then start to measure the driver's vital signs and transmit them to medical facilities, if necessary. If the system detects any unusual or serious health problems based on the medical findings<sup>10)11)</sup>, the system will automatically contact medical staff and summon rescue.



Fig. 11 Daily health check system. This figure shows one of the potential applications of our steering wheel sensor. The system automatically measures and stores a driver's vital signs, and reports the driver's condition as well as any potential risk to the driver's health, and will also summon rescue if necessary.

Fig. 12 shows how our system could be used to evaluate a driver's mental state. The driver's mental state is known to be an important factor affecting any assessment of driving capability<sup>12)</sup>, and should be maintained in a stable condition. The mental condition monitoring system shown in Fig. 12 measures the driver's vital signs and determines the driver's mental state: whether it is calm, stable, aroused, fired-up, anxious and so on.

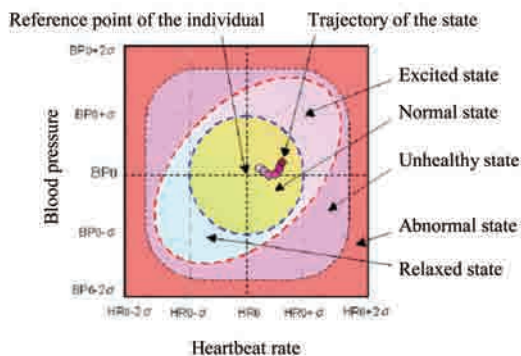


Fig. 12 Concept of a tracking system to monitor a driver's mental state

7. SUMMARY/CONCLUSIONS

We have developed a new vital signs sensor, which is built into the steering wheel and can measure the driver's electrocardiogram and pulse wave. Unlike conventional medical sensors, our system allows drivers to noninvasively monitor their vital signs just by gripping the steering wheel while driving, even when there are strong vibrations or other external disturbances. The main challenge we faced was to minimize SNR deterioration and waveform distortion caused by fluctuation in the contact force between the optical sensor and the driver's palm. We solved this problem by designing a new mounting mechanism that couples the optical sensor and the steering wheel with a spring. This mechanism successfully reduced contact fluctuation by up to 14%. We also developed a signal processing technique to recover a clean pulse waveform by employing ensemble averaging and using the heartbeat signal as a trigger. With the help of these new techniques, we successfully achieved an improvement in pulse wave quality of 27 dB in terms of SNR, from 15 to 42 dB under vehicle vibration of 0.65 m/s<sup>2</sup>. We also demonstrated the potential for using the pulse wave sensor to measure blood pressure, and obtained a very accurate estimation, with an error of less than 4.3 +/- 2.4 mmHg.

The limitation of this paper was the appearance of our sensor, which would tend to make drivers aware of its presence. In future work, we will develop concealed sensors such as a heartbeat sensor made of conductive fabric.

REFERENCES

- 1) Traffic accidents situation, National Police Agency, September, 2010, JAPAN
- 2) J. M. Goldman, M. T. Petterson, R. J. Kopotic, S. J. Barker, "MASIMO SIGNAL EXTRACTION PULSE OXIMETRY," Journal of Clinical Monitoring, vol.16, pp.475-483, 2000
- 3) H. J. Baek, H. B. Lee, J. S. Kim, J. M. Choi, etc., "Non-intrusive Biological Signal Monitoring in a Car to Evaluate a Driver's Stress and Health State," TELEMEDICINE and e-HEALTH, Vol.15, No.2, pp.182-189, 2009
- 4) Yamaguchi K., "Evaluation of fatigue by using acceleration plethysmography," Nippon Rinsho, Jun:65(6), 1034-42, 2007 (in Japanese)

- 5) Leif Sornmo, Pablo Laguna, "BIOELECTRICAL SIGNAL PROCESSING IN CARDIAC AND NEUROLOGICAL APPLICATIONS", ELSEVIER, ISBN 0-12-437552-9: 193-200, 2005
- 6) Crossbow Technology, Inc., "Products; NAV440," <http://www.xbow.com/defense-solutions/products/NAV440.html>, Dec. 2010
- 7) Wikipedia, "Signal to noise ratio," [http://en.wikipedia.org/wiki/Signal-to-noise\\_ratio](http://en.wikipedia.org/wiki/Signal-to-noise_ratio), Dec. 2010
- 8) A&D Company, Ltd., "Electronic sphygmomanometer; TM-2580," <http://www.aandd.co.jp/adhome/products/me/tm2580.html>, Dec. 2010 (in Japanese)
- 9) Wikipedia, "Stepwise regression," [http://en.wikipedia.org/wiki/Stepwise\\_regression](http://en.wikipedia.org/wiki/Stepwise_regression), Dec. 2010
- 10) Osaka M, Watanabe E, Murata H, Fuwamoto Y, Nanba S, Sakai K, Katoh T., "V-shaped trough in autonomic activity is a possible precursor of life-threatening cardiac events," *Circ J.* 74(9):1906-15, 2010
- 11) Kellett J, Deane B, Gleeson M., "Derivation and validation of a score based on Hypotension, Oxygen saturation, low Temperature, ECG changes and Loss of independence (HOTEL) that predicts early mortality between 15 min and 24 h after admission to an acute medical unit," *Resuscitation*, 78(1): 52-8, 2008
- 12) Dula CS, Geller ES., "Risky, aggressive, or emotional driving: addressing the need for consistent communication in research," *J Safety Res.* 34(5): 559-66 2003.

<著 者>



二ツ山 幸樹  
(ふたつやま こうき)  
研究開発3部 特定開発室ME  
医療用モニタ及びドライバモニタの技術開発に従事



光本 直樹  
(みつもと なおき)  
基礎研究所 先端研究  
次世代コンピュータ技術, 脳応用技術開発に従事



河内 泰司  
(かわち たいじ)  
研究開発3部 特定開発室ME  
医療用モニタ及びドライバモニタの技術開発に従事



中川 剛  
(なかがわ つよし)  
研究開発3部 特定開発室ME  
医療用モニタ及びドライバモニタの技術開発に従事